Accuracy of DSM By Using Unmanned Aerial Vehicles on the Downstream of Welang Riverbank, District of Pasuruan, Jawa Timur

By W D klahulan

Available online at
http://ojs.unik-kediri.ac.id/index.php/ukarst/index

U KaRsT

http://dx.doi.org/10.30737/ukarst.v3i2

Accuracy of DSM By Using Unmanned Aerial Vehicles on the Downstream of Welang Riverbank, District of Pasuruan, Jawa Timur

D. W. Khaulan [1*], E. Hidayah [2], G. Halik [3].

[1*,2,3] *Master Program in Civil Engineering, Department of Civil Engineering, Faculty of Engineering,*

University of Jember,

Jl. Kalimantan 37 Jember.

Email : [1*] dean.uptti@unej.ac.id

A R T I C L E   I N F O

A B S T R A C T

The Digital Surface Model (DSM) is commonly used in studies on flood map modelling. The lack of accurate, high-resolution topography data has hindered the flood modelling. The use of the Unmanned Aerial Vehicle (UAV) can help data acquisition with sufficient accuracy. The objective of this research is to provide high-resolution DSM generated maps by Ground Control Points (GCPs) settings. Improvement on the accuracy of the model was pursued by distributing 20 GCPs along the edges of the study area. Agrisoft software was used to generate the DSM. The generated DSM can be used for various planning purposes. The accuracy of the model is measured in Root Mean Square Error (RMSE) based on the generated DSM. The RMSE values are 0.488 m for x-coordinates and y-coordinates (horizontal direction) and 0.161 m for z-coordinates (vertical direction).

1. Introduction

To model a river flood, topography data with sufficiently high resolution are necessary to represent the geometric features of the river channels and floodplains [1], [2]. However, most areas vulnerable to floods are relatively flat. A DSM generates maps containing information on elevations of all features on the Earth surface [3], [4]. The information can then be used in the flood modeling [5]. An alternative way to improve the resolution of the DSM is by generating the DSM from an UAV imagery [6]. The approach of DSM generation from the UAV imagery emphasizes measurement effectiveness and accuracy [7]. It is capable of generating detailed spatial data [8], needs low cost and produces better results than DEM 30m SRTM does [9].

A number of studies has proposed ways to improve the accuracy of high-resolution DEM by using UAV imagery. The accuracy of the model can be improved by setting various variables, including the UAV flight design and the quality of the camera [10], [11], and the position of Ground Control Points [9], [12]. A previous study pursued accuracy improvement by setting the positions of Ground Control Points (GCPs) and increasing their numbers so that it resulted in low RMSE value, namely 6 cm [9]. Configuring the GCP distributions in the edges of the study area and applying stratified distribution also contributed to significant improvement on the accuracy [12], [13]. The use of GCPs is important in output verification so that photogrammetry with centimeter-level accuracy can be obtained [14].

To further improve the accuracy, many authors make the use of Agrisoft software. Jebur, Abed and Mohammed [15] used Agrisoft, and to validate the model, geometrical measurement of the shapes in the field was carried out by accurate object selection. Agrisoft shows good reliability and validation in triangulation process and in 3D modelling application. In addition, Agrisoft Photoscan software is easier to use that LPS software because Agrisoft does not need estimate values for unknown parameters, including exterior orientation parameters and control points [15].

The objective of this study is to provide high-resolution Digital Surface Model (DSM) data for flood hazard mapping in flat areas. To obtain good accuracy, the construction of the DSM makes the use of UAV imagery by setting the positions of GCP to be well distributed over the study area and to be densely located on the edges of the area. The accuracy of the resulted map is quantitatively computed in Root Mean Square Error (RMSE). The mapping was conducted on seven villages in the lower course of Welang River. These villages are located close to the beach.

2. Area of Study and Method

2.1. Area of Study

The study was conducted in the lower course of Welang River, District of Pasuruan, Province of East Java as seen in figure 1. The lower course of this river has relatively flat topography, making it vulnerable to floods. A previous flood at Welang River inundated thousands of houses [16]. The total area under study is 3.31 km^2 with land covers of housings, paddy fields, and plantation field. The elevation in this area varies from 0 m to 10 m above sea level.
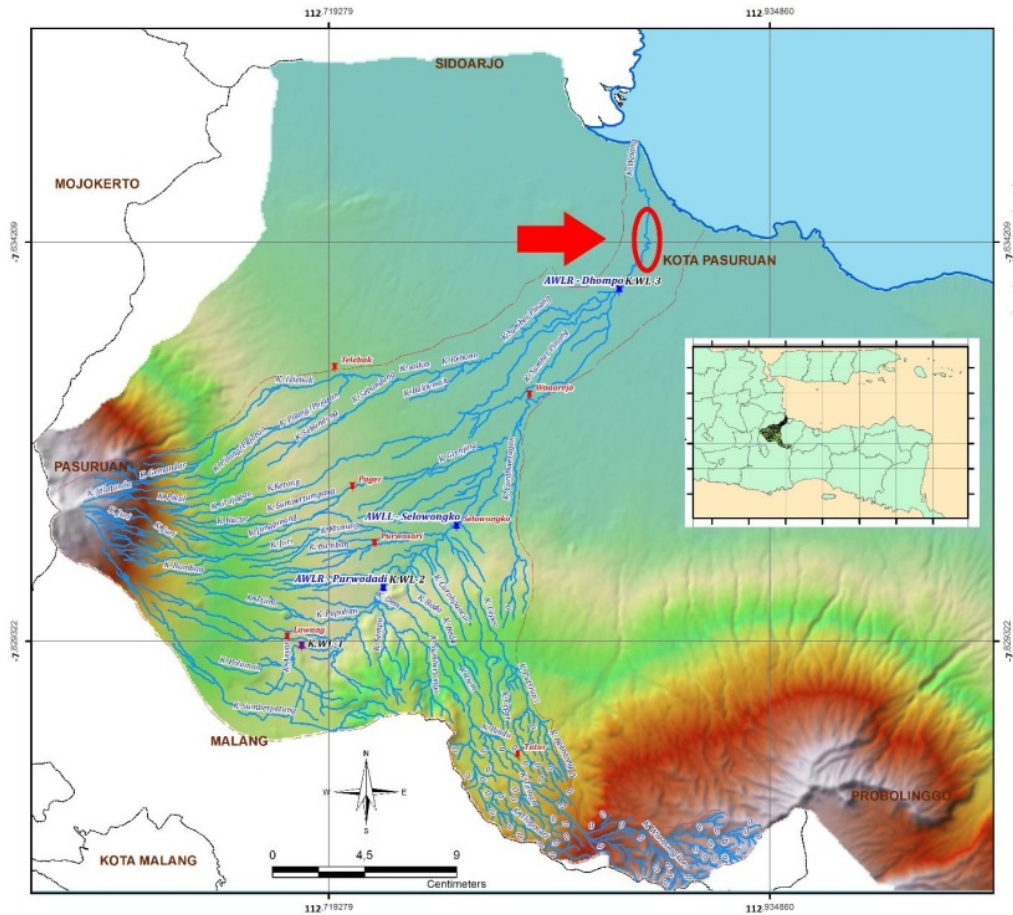
Source: UPT-PSDA Pasuruan (AutoCAD, 2020)

Figure 1. Map of the Area of Study

2.2. UAV Photogrammetry

A multi-rotor type (quadcopter) UAV, as seen in Figure 2, was used in this research. This kind of drone is commonly used in Indonesia for commercial, academic, and hobby purposes due to its relatively low cost. The UAV used in this study is a fourth-generation one, which has more sophisticated specifications than earlier generations do. Table 1 presents some of the specifications of the UAV. One of the installed features of the UAV is a forward sensor, which identifies obstacles in forward direction so that the UAV can avoid collision during forward movement.

Source: research document (Samsung note 4, 2020)

Figure 2. Quadcopter UAV technology

**Table 1.**   Specifications of the UAV and the camera used in the research

UAV Specification		Camera Specification	
Type	Quadcopter	Sensor	CMOS 1/2,3"
Weight	1380 gram (including propellers and batteries)	Lense	FOV 94° 20mm
Speed	20 m/s	Camera resolution	12.4 MP
Flight duration	28 minutes with Intelligent flight battery of 81.3 Wh/15.2 V	Photo resolution	4000x3000 pixel
Remote control transmission distance	3.5 km	Photo format	JPEG, DNG (RAW)

Source : http://www.dji.com/phantom-4/info#specs

2.3. Settings of GCPs

The GCPs have been used to improve the accuracy of the DSM. The GCPs were distributed over the study area [11], densely located in the edges of the area to minimize the total error [12]. In this study, prior to the UAV flight, twenty GCPs had been located in the area, as shown in Figure 3. The data were collected by using a L1-static GPS on the land surface. The selected locations of the GCPs were permanent landmarks such as a road-corner building,

a bridge corner, or other buildings in the area. The marks for the GCPs were painted with bright and very reflective colours, and they were well distributed in the study area. This approach was chosen to get coordinate points that can be used to assess the accuracy of the data. Leica GPS used in this research has nominal accuracy of 1 m at each of x -coordinates and y-coordinates, and 2 m at z-coordinates.
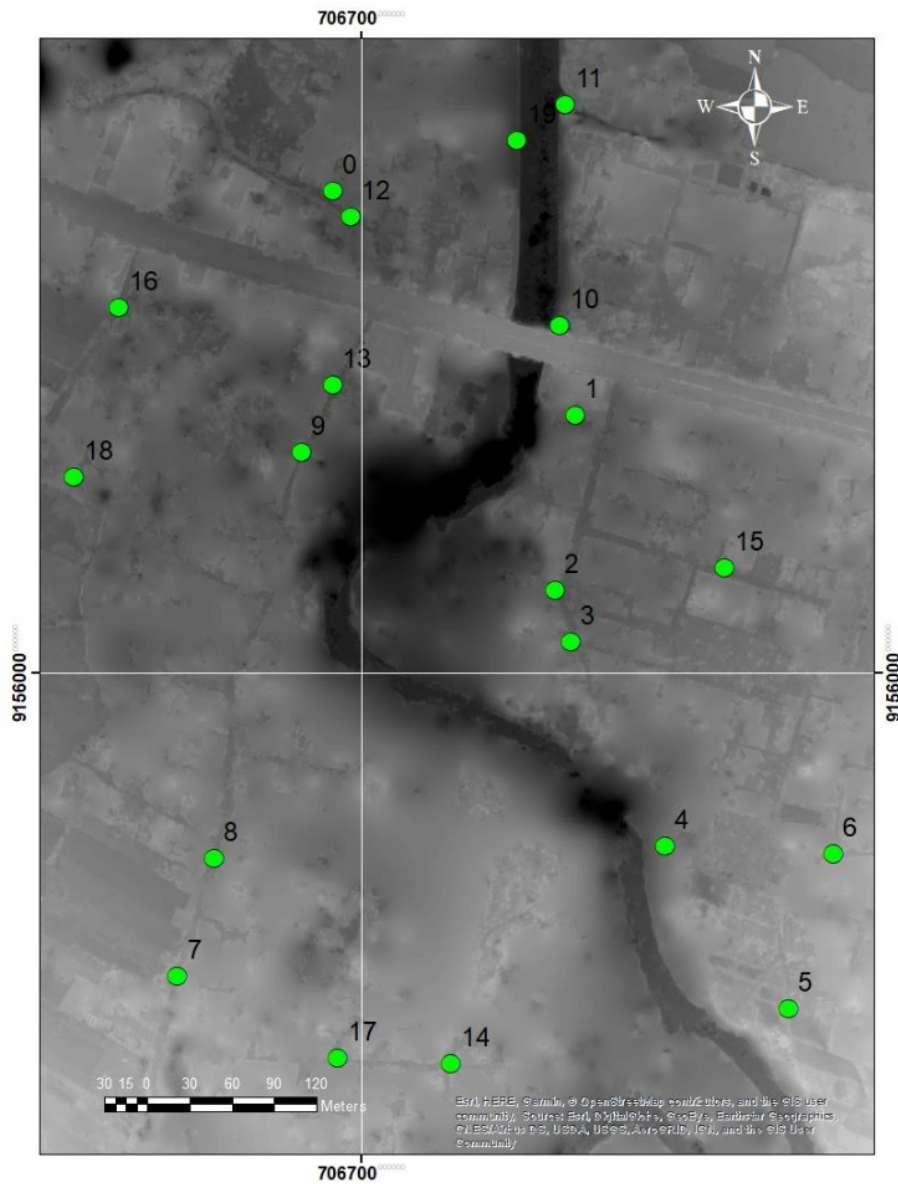
Source: Research document (Arc- GIS, 2020)

Figure 3. Positions of Ground Control Points

2.4.   DSM Map Construction

Construction of the DSM map is conducted in Agrisoft Photoscan Professional software package version 1.2.5. Agrisoft uses algorithms that has achieved significant accuracy in DSM [15]. The framework of the map construction consists of three steps. The first step was photo alignment based on feature identification and feature matching. In the photo alignment step, the software estimated the orientation of the camera external and internal parameters, including nonlinear radial distortion. The software also estimated the required focal length, which was then extracted from metadata. The results of this step were photo positions aligned for each image, internal calibration parameters, and coordinate points. In the second step, the coordinate system in the reference settings of the sparse point cloud was set to local coordinate system (WGS84 UTM with 49S zone), and the the surface type parameter of dense point cloud was set to *height field*, in accordance to the GCPs. The third step was to get the mesh exported to DSM grid. The DSM was then used as the basis for orthorectification to produce an orthomosaic.

2.5.   Accuracy Assessment

The quality of a DSM is assessed based on the accuracy of each pixel, referred to as the absolute accuracy, and the accuracy of displayed morphology, referred to as the relative accuracy, which is expressed in RMSE values [9], [17]. The RMSE values are computed based on the discrepancy between the observed coordinate values and the reference coordinate values. The horizontal accuracy is measured from x-coordinates and y-coordinates, and the vertical accuracy is measured from z-coordinates. Equations (1)-(3) are RMSE formulas that indicate horizontal accuracy, and equations (4)-(5) are RMSE formulas that indicate vertical accuracy.

$$RMSEx \quad = \sqrt{\frac{\sum_{i=1}^{n}(x_{oi}-x_{ri})^2}{n}} \qquad (1)$$

$$RMSEy \quad = \sqrt{\frac{\sum_{i=1}^{n}(y_{oi}-y_{ri})^2}{n}} \qquad (2)$$

$$RMSExy \quad = \sqrt{\frac{\sum_{i=1}^{n}[(x_{oi}-x_{ri})^2+(y_{oi}-y_{ri})^2]}{n}} \qquad (3)$$

$$RMSEz \quad = \sqrt{\frac{\sum_{i=1}^{n}(z_{oi}-z_{ri})^2}{n}} \qquad (4)$$

$$RMSEt \quad = \sqrt{\overline{RMSE_{xy}}^2 + (RMSE_z)^2} \qquad (5)$$

With n is the number of points; x_{oi} and y_{oi} are x-coordinate and y-coordinate, respectively, that represent i-th observation (i.e. orthophoto) of the CP; x_{ri} and y_{ri} are x-coordinate and y-coordinate, respectively, that represent i-th reference (i.e. L1-static GPS measurement) of the CP. For the vertical direction, z_{oi} is the z elevation coordinate that represents i-th   DSM of the CP, and z_{ri} is the z elevation coordinate that represents i-th reference (i.e. L1-static GPS measurement) of the CP.

The accuracy level of the resulted map is aimed at conforming the DSM standard accuracy that has been issued by the Indonesian Geospatial Information Agency (Badan Informasi Geospasial, BIG) [18]. According to the standard, the accuracy of x-coordinate positions and y-coordinate positions should be measured based on CE90 values, and the resolution of z-coordinate positions should be measured based on LE90. The CE90 values, associated with horizontal positions, are computed as 1.5175 times the RMSE of horizontal positions. The LE90, associated with vertical positions, are computed as 1.6499 times the RMSE of vertical positions.

## 3. Results and Discussion

3.1.   Resulted DSM Map

Based on IDW interpolation in Agisoft Photoscan software, 738 aligned images of the UAV (as shown in Figure 4) were exported to generate a DSM map of the study area.
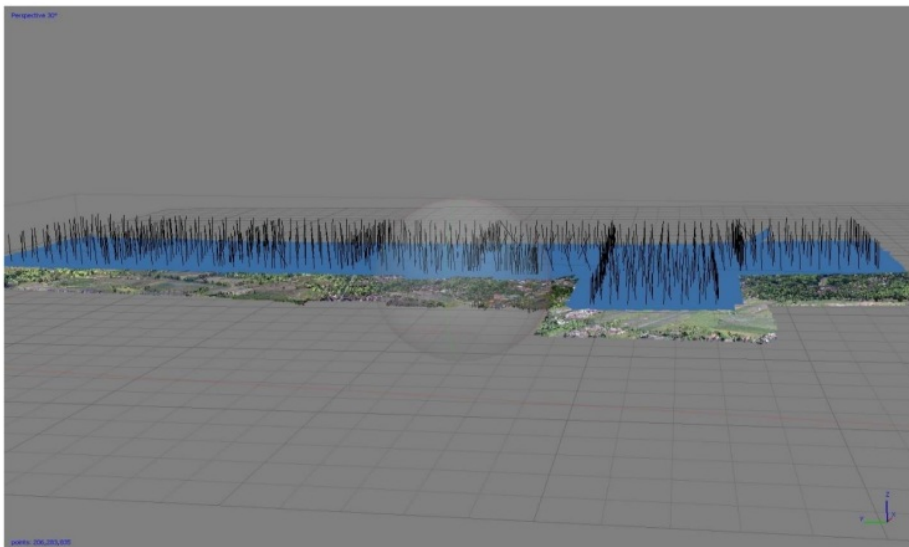
Source: Research document (Photoscan software, 2020)

Figure 4. 738 Aligned Images from the UAV Imagery

The resulted DSM map is shown in Figure 5. The results of the DSM map, which are compared qualitatively with satellite imagery maps, show that in the red circle there is an alignment and continuity between the road lines in the province, village roads and railways. This shows that there is qualitative accuracy.
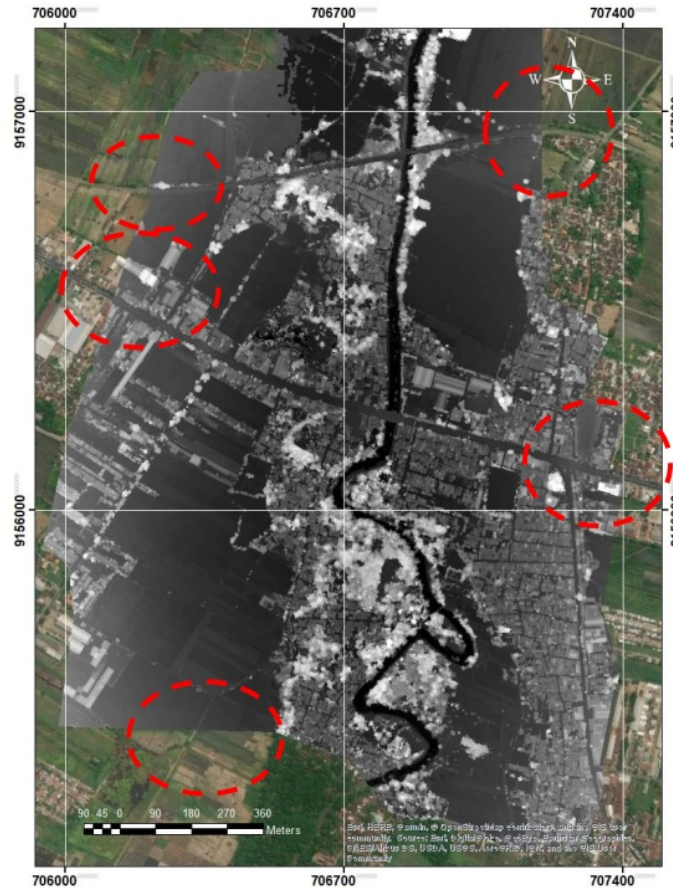
Source: Research document (Arch Gis, 2020)

Figure 5. DSM of the Area of Study

3.2. Accuracy of the DSM

Table 1 shows the values for the horizontal and vertical. The computed values of RMSE determine the quantitative accuracy of the generated DSM. RMSE values are computed from the square difference between observed coordinate values and reference coordinate values at each of 20 GCPs positions. The resulted RMSEy, computed from the sum of the square difference between the GCPs with North coordinates of observations (i.e. orthophotos) and North coordinates of the references (i.e. L1-static GPS measurement), is 0.455 m. The resulted

RMSEx, computed from the sum of the square difference between the GCPs with East coordinates of observations (i.e. orthophotos) and East coordinates of the references (i.e. L1-static GPS measurement), is 0.488 m. The resulted RMSExy, computed by using equation (3), is 0.667 m. The resulted RMSEz is 0.161 m. It is computed from the sum of the square difference between of GCPs coordinates with observed elevations (i.e. orthophotos) and coordinates of the references (i.e. L1-static GPS measurement). The resulted $RMSE_T$ is 0.686 m. It is computed from RMSExy and RMSEz as in Equation (5). The observed coordinate points and the reference coordinate points are presented in Table 2. The resulted RMSEs are presented in Table 3.

Table 2. Horizontal and Vertical Coordinate Points

QC POIN	Reference Coordinate Points, i.e. L1-Static Measurement (m)			Observed Coordinate Points, i.e. Orthopotos (m)		
	X	Y	Z	X	Y	Z
1	706976.70	9155705	12.04	706976.20	9155704	12.14
2	706980.12	9155708	10.08	706980.97	9155708	10.21
3	706984.90	9155712	7.68	706984.86	9155713	7.73
4	706988.92	9155717	8.98	706988.08	9155716	8.64
5	706994.07	9155720	12.71	706994.58	9155720	12.89
6	706989.43	9156395	16.46	706989.05	9156396	16.63
7	706983.64	9156395	12.55	706983.10	9156396	12.49
8	706988.83	9156395	12.40	706988.10	9156394	12.51
9	706987.52	9156395	12.06	706987.16	9156395	12.53
10	706987.00	9156395	12.90	706987.20	9156395	12.87
11	706384.44	9155545	11.39	706384.92	9155546	11.39
12	706947.55	9155755	10.83	706947.95	9155754	10.87
13	706914.57	9155877	6.13	706914.61	9155878	6.14
14	706472.23	9155943	10.35	706472.23	9155942	10.46
15	706847.46	9156022	6.76	706847.94	9156023	6.68
16	706837.91	9156059	6.83	706837.35	9156059	6.71
17	706423.26	9156156	8.12	706423.54	9156156	8.28
18	706852.78	9156183	7.28	706852.17	9156184	7.28
19	706679.68	9156338	7.99	706679.26	9156339	7.87
20	706855.57	9157148	11.46	706855.21	9157147	11.44

Source: Jember University of Hydro-Technik Laboratory of (2020)

Table 3.   RMSE Values of Horizontal and Vertical Coordinate Points

Root Mean Square Error (RMSE) Validation Points
$RMSE_x = 0.488$ m
$RMSE_y = 0.455$ m
$RMSE_{xy} = 0.667$ m
$RMSE_z = 0.161$ m
$RMSE_T = 0.686$ m

Source: Jember University of Hydro-Technik Laboratory of (2020)

The computed RMSE for z (i.e. vertical direction) is 0.161 m. By using UAVs with the same specification as the one used in this study, Akturk [9] studied 0.55 km^2 area by using 14 GCPs and the resulted $RMSE_z$ was 0.51 m; Nagendran [14] studied 2.43 km^2 area by using 16 GCPs and the resulted $RMSE_z$ was 0.31 m; the study of Azmi [17] resulted in $RMSE_x$ value of 0.263 m, $RMSE_y$ value of 0.412 m, and $RMSE_z$ value of 0.704 m. Compared to the previous studies that used the DJI UAVs Phanthom 3-4 series [9], [14], [17], the horizontal accuracy of this study is low, whereas the vertical accuracy of this study is high, even though the size of the mapped area in this study is bigger than those of the previous studies.   It is likely that the significant vertical accuracy in this study is a result of the GCP positioning in which the GCPs were well distributed on the study area, particularly in the edges of the area. On the other hand, the errors in horizontal direction in this study are probably because the GPS used in this study was not geodetic one. In addition, the ratio between the number of GCPs and the total measured area in this study is smaller than the ratios in the previous studies [9], [14], [17]. In principle, inaccuracies in the use of UAVs depend on multifactors, such as the types of aircrafts, sensors [10], operating systems, and processing software [19].

Following computation method of the standard accuracy of Indonesian Geospatial Information Agency, it is found that on 90% confidence level, the resulted CE90 and LE90 values are 1.474 m and 0.265 m, as presented in Table 4. Therefore, based on the standard horizontal accuracy of the BIG for a base map, the class of the horizontal of the resulted map are Class 1 in 1:5000 scale, whereas the class of the vertical accuracy of the resulted map is Class 1 in 1:2500 scale. These results show that the resulted data in this study are suitable to be used in flood hazard planning. Flood hazard mapping for the areas in the lower course of a river is an example of the DSM implementation [5], [20], [21]. Flood inundation areas are characterized by damaged topography, relatively plain, and rich of trees, so that availability of UAV imagery is extremely helpful to generate DSM for the areas.

Table 4.   DSM Accuracy and BIG Standard Accuracy

Accuracy	Test Result (m)	BIG Standard Accuracy at Scale of 1:5000		
		Class 1 (m)	Class 2 (m)	Class 3 (m)
Horizontal (CE90)	1.474	1.5	3	4.5
		BIG Standard Accuracy at Scale of 1:2500		
		Class 1 (m)	Class 2 (m)	Class 3 (m)
Vertical (LE90)	0.265	0.5	0.75	1.0

Source: Jember University of Hydro-Technik Laboratory of (2020)

4. Conclusion and Suggestion

4.1. Conclusion

The DJI Phantom UAV DJI is good to be used for small-scale mapping. The resulting DSM map has qualitative accuracy, which indicates a continuity and parallels to the satellite image map of road and railroad indicators. Geometric accuracy from this study found that, the computed RMSE at x and y (i.e. horizontal direction) are 0.488 m and 0.455 m, respectively. Based on the BIG standard, the horizontal geometric accuracy is 1,474 m which is suitable for 1: 5000 scale mapping of orthophoto mosaic data, while the vertical accuracy is 0.264 m which is included on the 1: 2,500 scale maps of the DSM data. This map can be used to recognize special features and details. Qualitative and quantitative (geometric) accuracy is quite detailed when used as input for modeling and mapping of coastal flood disasters

4.2. Suggestion

It is advised for future studies, in order to achieve better accuracy, to use more advanced UAV system, to improve consideration on GCP positioning, and to use GPS that is both geodetic and real-time kinematic.

5. Acknowledgments

References

[1]   S. Saksena and V. Merwade, 'Incorporating the effect of DEM resolution and accuracy for improved flood inundation mapping', *J. Hydrol.*, vol. 530, pp. 180–194, 2015, doi: 10.1016/j.jhydrol.2015.09.069.

[2]   J. Vesakoski, P. Alho, J. Hyyppä, M. Holopainen, C. Flener, and H. Hyyppä, 'Nationwide Digital Terrain Models for Topographic Depression Modelling in Detection of Flood Detention Areas', pp. 271–300, 2014, doi: 10.3390/w6020271.

[3]   I. Indarto and D. Prasetyo, 'Pembuatan Digital Elevation Model Resolusi 10m dari Peta RBI dan Survei GPS dengan Algoritma ANUDEM', *J. Keteknikan Pertan.*, vol. 2, no. 1, p. 21955, 2014.

[4]   A. N. Safi'i and P. Hartanto, 'Pembuatan Digital Terrain Model (DTM) dari Light Detection and Ranging (LiDAR) menggunakan Metode Morfologi Sederhana', *Teknik*, vol. 40, no. 1, p. 40, 2019, doi: 10.14710/teknik.v40i1.23004.

[5]   S. Mourato, P. Fernandez, L. Pereira, and M. Moreira, 'Improving a DSM Obtained by Unmanned Aerial Vehicles for Flood Modelling', *IOP Conf. Ser. Earth Environ. Sci.*, vol. 95, no. 2, 2017, doi: 10.1088/1755-1315/95/2/022014.

[6]   A. Jebur, F. M. Abed, and M. U. Mohammed, '3D City Modelling by Photogrammetric Techniques', no. July 2019, 2017, doi: 10.13140/RG.2.2.11494.06722.

[7]   N. Arsyad, 'Akurasi Citra data Foto Udara Persimpangan Lalu Lintas Kota Kendari', *Rekayasa Sipil*, vol. 14, no. 1, pp. 51–59, 2020.

[8]   R. Meiarti, T. Seto, and J. Sartohadi, 'Uji Akurasi Hasil Teknologi Pesawat Udara Tanpa Awak (Unmanned Aerial Vehicle) Dalam Aplikasi Pemetaan Kebencanaan Kepesisiran', *J. Geogr. Edukasi dan Lingkung.*, vol. 3, no. 1, p. 1, 2019, doi: 10.29405/jgel.v3i1.2987.

[9]   E. Akturk and A. O. Altunel, 'Accuracy assesment of a low-cost UAV derived digital elevation model (DEM) in a highly broken and vegetated terrain', *Meas. J. Int. Meas. Confed.*, vol. 136, no. February 2019, pp. 382–386, 2019, doi: 10.1016/j.measurement.2018.12.101.

[10] A. R. Yusoff, M. F. Mohd Ariff, K. M. Idris, Z. Majid, and A. K. Chong, 'Camera calibration accuracy at different UAV flying heights', *Int. Arch. Photogramm. Remote Sens. Spat. Inf. Sci. - ISPRS Arch.*, vol. 42, no. 2W3, pp. 595–600, 2017, doi: 10.5194/isprs-archives-XLII-2-W3-595-2017.

[11] E. Sanz-Ablanedo, J. H. Chandler, J. R. Rodríguez-Pérez, and C. Ordóñez, 'Accuracy of Unmanned Aerial Vehicle (UAV) and SfM photogrammetry survey as a function of the number and location of ground control points used', *Remote Sens.*, vol. 10, no. 10, 2018, doi: 10.3390/rs10101606.

[12] P. Martínez-Carricondo, F. Agüera-Vega, F. Carvajal-Ramírez, F. J. Mesas-Carrascosa, A. García-Ferrer, and F. J. Pérez-Porras, 'Assessment of UAV-photogrammetric mapping accuracy based on variation of ground control points', *Int. J. Appl. Earth Obs. Geoinf.*, vol. 72, no. May, pp. 1–10, 2018, doi: 10.1016/j.jag.2018.05.015.

[13] V. Casella, F. Chiabrando, M. Franzini, and A. M. Manzino, 'Accuracy assessment of a UAV block by different software packages, processing schemes and validation strategies', *ISPRS Int. J. Geo-Information*, vol. 9, no. 3, 2020, doi: 10.3390/ijgi9030164.

[14] S. K. Nagendran, W. Y. Tung, and M. A. Mohamad Ismail, 'Accuracy assessment on low altitude UAV-borne photogrammetry outputs influenced by ground control point at different altitude', *IOP Conf. Ser. Earth Environ. Sci.*, vol. 169, no. 1, 2018, doi: 10.1088/1755-1315/169/1/012031.

[15] A. Jebur, F. Abed, and M. Mohammed, 'Assessing the performance of commercial Agisoft PhotoScan software to deliver reliable data for accurate3D modelling', *MATEC Web Conf.*, vol. 162, 2018, doi: 10.1051/matecconf/201816203022.

[16] M. A.- DetikNews, '8.740 Rumah di 9 Desa/Kelurahan di Pasuruan Terendam Banjir', [Online]. Available: https://news.detik.com/berita-jawa-timur/d-3880153/8740-rumah-di-9-desakelurahan-di-pasuruan-terendam-banjir.

[17] S. M. Azmi, B. Ahmad, and A. Ahmad, 'Accuracy assessment of topographic mapping using UAV image integrated with satellite images', *IOP Conf. Ser. Earth Environ. Sci.*, vol. 18, no. 1, 2014, doi: 10.1088/1755-1315/18/1/012015.

[18] Badan Informasi Geospasial, *PERATURAN BADAN INFORMASI GEOSPASIAL NOMOR 6 TAHUN 2018*. 2018.

63 - 63

Ukarst : Universitas Kadiri Riset Teknik Sipil.
Volume 5 Number 1, (2021).

[19] G. Popescu, D. Iordan, and V. Păunescu, 'The Resultant Positional Accuracy for the Orthophotos Obtained with Unmanned Aerial Vehicles (UAVs)', *Agric. Agric. Sci. Procedia*, vol. 10, pp. 458–464, 2016, doi: 10.1016/j.aaspro.2016.09.016.

[20] E. Yalcin, 'Two-dimensional hydrodynamic modelling for urban flood risk assessment using unmanned aerial vehicle imagery: A case study of Kirsehir, Turkey', *J. Flood Risk Manag*., vol. 12, no. S1, pp. 1–14, 2019, doi: 10.1111/jfr3.12499.

[21] C.-G. Jung and S.-J. Kim, 'Comparison of the Damaged Area Caused by an Agricultural Dam-Break Flood Wave Using HEC-RAS and UAV Surveying', *Agric. Sci*., vol. 08, no. 10, pp. 1089–1104, 2017, doi: 10.4236/as.2017.810079.

Accuracy of DSM By Using Unmanned Aerial Vehicles on the Downstream of Welang Riverbank, District of Pasuruan, Jawa Timur

ORIGINALITY REPORT

22%

SIMILARITY INDEX

PRIMARY SOURCES

1 Amy Wadu, A A Tuati, M R Sodanango. "Strategy To Reduce Traffic Jams On Piet A. Tallo Street, Kupang City", UKaRsT, 2020
Crossref

258 words — 6%

2 www.mdpi.com
Internet

116 words — 2%

3 Luana Mendes dos Santos, Gabriel Araujo e Silva Ferraz, Brenon Diennevan de Souza Barbosa, Adriano Valentim Diotto et al. "Determining the Leaf Area Index and Percentage of Area Covered by Coffee Crops Using UAV RGB Images", IEEE Journal of Selected Topics in Applied Earth Observations and Remote Sensing, 2020
Crossref

45 words — 1%

4 Daniela Ali-Sisto, Ranjith Gopalakrishnan, Mikko Kukkonen, Pekka Savolainen, Petteri Packalen. "A method for vertical adjustment of digital aerial photogrammetry data by using a high-quality digital terrain model", International Journal of Applied Earth Observation and Geoinformation, 2020
Crossref

38 words — 1%

5 ejournal.undip.ac.id
Internet

34 words — 1%

6 www.diva-portal.org
Internet

30 words — 1%

7 Layla A. Mohammed, Saleh I. Khassaf, Kareem R. Al-Murshidi.

"Application HEC-RAS Model to Simulate the Flood Wave Due to Dam Failure", 2019 4th Scientific International Conference Najaf (SICN), 2019
Crossref

29 words — 1%

8 D. Bolkas, B. Naberezny, M. G. Jacobson. "Comparison of sUAS Photogrammetry and TLS for Detecting Changes in Soil Surface Elevations Following Deep Tillage", Journal of Surveying Engineering, 2021
Crossref

28 words — 1%

9 Quang Minh Nguyen, Thi Thu Huong Nguyen, Phu Hien La, Hugh G. Lewis, Peter M. Atkinson. "Downscaling Gridded DEMs Using the Hopfield Neural Network", IEEE Journal of Selected Topics in Applied Earth Observations and Remote Sensing, 2019
Crossref

28 words — 1%

10 digilib.gmu.edu
Internet

27 words — 1%

11 www.jurnal.unsyiah.ac.id
Internet

26 words — 1%

12 H.T. Samboko, I. Abas, W.M.J. Luxemburg, H.H.G. Savenije, H. Makurira, K. Banda, H.C. Winsemius. "Evaluation and improvement of remote sensing-based methods for river flow management", Physics and Chemistry of the Earth, Parts A/B/C, 2020
Crossref

24 words — 1%

13 Serkan Biçici, Mustafa Zeybek. "An approach for the automated extraction of road surface distress from a UAV-derived point cloud", Automation in Construction, 2021
Crossref

24 words — 1%

14 Umair Iqbal, Pascal Perez, Wanqing Li, Johan Barthelemy. "How Computer Vision can Facilitate Flood Management: A Systematic Review", International Journal of Disaster Risk Reduction, 2021
Crossref

24 words — 1%

www.utu.fi

| 15 | Internet | 24 words — 1% |

M Ihsan, L Somantri, N T Sugito, S Himayah, A R Affriani. "The Comparison of Stage and Result Processing of Photogrammetric Data Based on Online Cloud Processing", IOP Conference Series: Earth and Environmental Science, 2019
Crossref
16 — 23 words — < 1%

rekayasasipil.ub.ac.id
Internet
17 — 22 words — < 1%

www.neliti.com
Internet
18 — 21 words — < 1%

A Jayanegara, B Wardiman, M Kondo, M Ridla, Nahrowi, E B Laconi. "Fermentative quality of silage as affected by protein level in the ensiled material: A meta-analysis", IOP Conference Series: Earth and Environmental Science, 2020
Crossref
19 — 16 words — < 1%

Patricio Martínez-Carricondo, Francisco Agüera-Vega, Fernando Carvajal-Ramírez, Francisco-Javier Mesas-Carrascosa et al. "Assessment of UAV-photogrammetric mapping accuracy based on variation of ground control points", International Journal of Applied Earth Observation and Geoinformation, 2018
Crossref
20 — 16 words — < 1%

"GCEC 2017", Springer Science and Business Media LLC, 2019
Crossref
21 — 16 words — < 1%

M.Deny Irawan Budianto, Zulkifli Lubis. "ALTERNATIF PENGGUNAAN AGREGAT HALUS BATU KAPUR MANTUP DALAM CAMPURAN ASPAL PANAS AC-WC", UKaRsT, 2020
Crossref
22 — 16 words — < 1%

jurnal.unej.ac.id
23

Internet
14 words — < 1%

24 O'Neill, N. T., A. R. Kalinauskas, J. D. Dunlop, A. B. Hollinger, H. Edel, M. Casey, and J. Gibson. "<title>Bathymetric Analysis Of Geometrically Corrected Imagery Data Collected Using A Two Dimensional Imager</title>", Ocean Optics VIII, 1986.
Crossref
13 words — < 1%

25 www.int-arch-photogramm-remote-sens-spatial-inf-sci.net
Internet
12 words — < 1%

26 www.erickunto.com
Internet
10 words — < 1%

27 www.tandfonline.com
Internet
10 words — < 1%

28 "Understanding and Reducing Landslide Disaster Risk", Springer Science and Business Media LLC, 2021
Crossref
10 words — < 1%

29 news.detik.com
Internet
9 words — < 1%

30 Benjamin U. Meinen, Derek T. Robinson. "Where did the soil go? Quantifying one year of soil erosion on a steep tile-drained agricultural field", Science of The Total Environment, 2020
Crossref
9 words — < 1%

31 iphrdefenders.net
Internet
9 words — < 1%

32 Lynne M. Rouse, Jan Krumnow. "On the fly: Strategies for UAV-based archaeological survey in mountainous areas of Central Asia and their implications for
8 words — < 1%

landscape research", Journal of Archaeological Science: Reports, 2020
Crossref

33   hess.copernicus.org
     Internet   8 words — < 1%

34   Saleem, Huq, Twumasi, Javed, Sajjad. "Parameters   8 words — < 1%
     Derived from and/or Used with Digital Elevation
     Models (DEMs) for Landslide Susceptibility Mapping and
     Landslide Risk Assessment: A Review", ISPRS International
     Journal of Geo-Information, 2019
     Crossref

35   www.ijert.org
     Internet   8 words — < 1%

36   Suhaila Hashim, Ernieza Suhana Mokhtar, Ahmad   6 words — < 1%
     Ikhwan Abdul Halim, Wan Mohd Naim Wan Mohd,
     Nor Aizam Adnan, Biswajeet Pradhan. "Cross Section Intervals of
     Flood Intervals of Flood Inundation Mapping at Ungauged Area",
     IOP Conference Series: Earth and Environmental Science, 2021
     Crossref